Japanese Journal of Applied Physics **54**, 070305 (2015) **RAPID COMMUNICATION**
http://dx.doi.org/10.7567/JJAP.54.070305

Defects in ZnO nanoparticles laser-ablated in water–ethanol mixtures at different pressures

Taku Goto[1], Mitsuhiro Honda[2], Sergei A. Kulinich[2,3*], Yoshiki Shimizu[4], and Tsuyohito Ito[1*]

[1]*Center for Atomic and Molecular Technologies, Graduate School of Engineering, Osaka University, Suita, Osaka 565-0871, Japan*
[2]*Institute of Innovative Science and Technology, Tokai University, Hiratsuka, Kanagawa 259-1292, Japan*
[3]*Aston Institute of Photonic Technologies, Aston University, Birmingham B4 7ET, U.K.*
[4]*Nanomaterials Research Institute, National Institute of Advanced Industrial Science and Technology (AIST), Tsukuba, Ibaraki 305-8565, Japan*
E-mail: skulinich@tokai-u.jp; tsuyohito@ppl.eng.osaka-u.ac.jp

Received April 24, 2015; accepted May 25, 2015; published online June 16, 2015

The effect of liquid medium and its pressure on the photoluminescence of ZnO nanoparticles prepared via laser ablation of Zn targets in various water–ethanol mixtures is studied. As the ethanol content increases, the photoluminescence of the product changes, while metallic zinc is observed to emerge in nanomaterials prepared in ethanol-rich environments. The applied pressure had a less profound effect, mainly affecting materials produced in water or water–ethanol, and much less those generated in pressurized ethanol. Tuning the reactivity of the liquid and pressurizing it during laser ablation is demonstrated to be promising for tailoring the emission properties of the product.

Recently, ZnO has been one of the most studied semiconductor materials with countless potential applications in optoelectronics, nanotechnology, biomedicine, energy conversion and other related fields.[1–21] Various nanostructures of ZnO have been synthesized via solvothermal approaches,[3,6,7,11] CVD,[6,15] microwave irradiation,[19] as well as laser ablation in liquid (LAL) media,[4,5,16,17,20–27] to name just a few techniques. The latter method, LAL, has recently become a very convenient, simple and versatile approach to prepare diverse nanomaterials at the laboratory scale.[4,16,17,20–29] In this approach, a solid target immersed into a liquid medium is typically ablated by a focused laser beam, which makes it possible to prepare nanomaterials using minimum amounts of solvents and nominally at room temperature, while the chemistry, morphology and size of the product are governed by the liquid, target and laser parameters used.[4,16,17,20–29] In addition, the recent use of high pressure (i.e., ablating in cells with pressurized liquid media) seems to extend the capability of this preparation technique to control the product properties.[5,25,30,31]

Though quite extensive studies have been conducted on ZnO nanomaterials prepared via LAL, there is no complete understanding of how such structures form and how to control their morphology, size and optical properties, for instance, photoluminescence (PL). This can be explained by using different laser parameters in different research groups, as well as using mainly neat water (sometimes with surfactants) as liquid medium.[5,16,17,20,23,25,27] The information on ZnO nanoparticles (NPs) prepared in organic media is very scarce.[21,24,26] The effect of medium pressure on ZnO NPs was only studied in water, revealing smaller NPs formed at higher pressures.[5,25] In this work, ZnO NPs are systematically prepared in water–ethanol mixtures and at different pressures using laser beam with fixed parameters. The products are then analyzed by several techniques, with a special focus on their PL properties, which are well-known to be closely related to various defects in such NPs.

The NPs were prepared in various water–ethanol mixtures, both at ambient pressure and pressurized in the chamber previously described elsewhere.[5,30] Zinc metal plates (99.9%) were ablated by a second harmonic (532 nm) of a Nd:YAG pulsed laser (Continuum Surelite) with a repetition rate of 10 Hz, pulse width of 5 ns, and fluence of ~30 mJ/pulse. The laser was focused on the Zn target by using a lens with a focal length of 3 cm. The target was fixed inside the high-pressure chamber, so that the incident angle of the laser beam (coming in through a sapphire window) was ~45°. The as-prepared colloids were cast on Si wafers and dried naturally, after which they were analyzed by X-ray diffraction (XRD) and PL spectroscopy. The latter PL measurements were conducted at room temperature with a He–Cd laser (325 nm) as excitation source. The products were also evaluated by transmission electron microscopy (TEM), and results generally consistent with the previously published research[5] were observed. Irrespective of the ethanol content in liquid media, most of prepared NPs had their sizes between 10 and 40 nm. Separate larger NPs of 100–150 nm in diameter were occasionally seen in products prepared at atmospheric pressure, which was previously observed for ZnO samples LAL-produced in pure water.[5] While only ZnO NPs were prepared in water, those prepared in ethanol and with bigger sizes often demonstrated crystal lattice of metallic Zn.

Figure 1 shows XRD patterns of NPs synthesized at atmospheric pressure (1 atm) in several water–ethanol media with ethanol concentration from 0 to 99.5 vol %. Peaks indicated by gray circles and blue squares correspond to the wurtzite ZnO and metallic Zn, respectively. The patterns clearly show that the majority of the products are wurtzite ZnO NPs, which agrees well with the previous reports,[5,16,17,25,27,32] while at higher ethanol concentrations ($\geq$ 60 vol %) in the media peaks of metallic Zn gradually emerge. The relative peak intensity of the Zn phase is stronger in the products prepared in ethanol-rich liquid media, indicating higher contents of metallic Zn in NPs prepared in media with 75–99.5 vol % of ethanol. This finding can be explained by the lower oxidation capability of ethanol in comparison with water and generally agrees well with the results previously published by Niu and coauthors who reported on NPs with metal cores and oxide (or sulfide) shells when a liquid with low oxidation potential was applied.[24,26]

The results of PL analysis are shown in Fig. 2(a) where normalized spectra for NPs prepared at 1 atm and in eight liquid mixtures with different composition are presented. It is clearly seen that the ethanol concentration in the liquid affects the nature of prepared NPs, which is mainly seen as (i) the intensity change in the UV range around 370 nm and (ii) a shift of the broad visible emission at different ethanol concentrations.

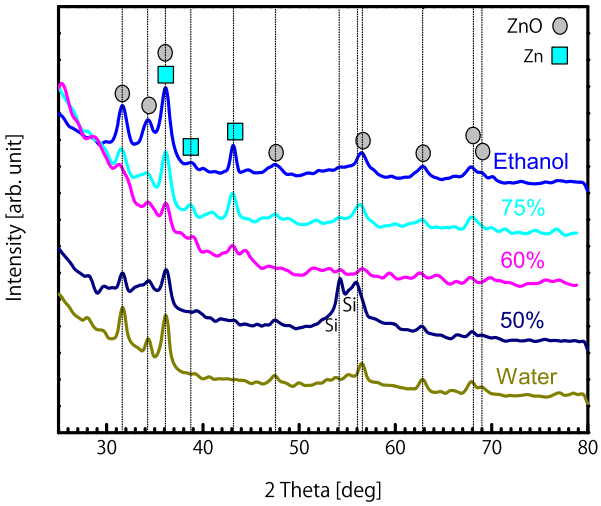

Fig. 1. (Color online) XRD patterns of samples prepared via ablation of metal Zn in water–ethanol mixtures at 1 atm (with ethanol concentration of 0, 50, 60, 75, and 99.5 vol %, from bottom to top). The peaks at ~54° are from Si substrates, while the other peaks were indexed as those of wurtzite ZnO (gray circles) or metallic Zn (blue squares).

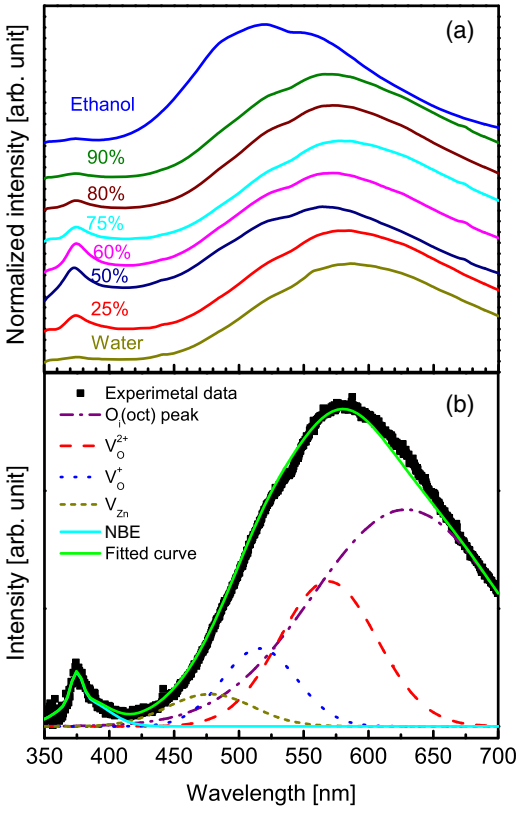

Fig. 2. (Color online) (a) Normalized photoluminescence spectra of samples prepared via ablation of metal Zn in water–ethanol mixtures at 1 atm (with ethanol concentration of 0, 25, 50, 60, 75, 80, 90, and 99.5 vol %, from bottom to top). (b) Example of multi-Gaussian curve-fitting, sample prepared in liquid with 75 vol % of ethanol at 1 atm. Black squares represent experimental data and solid green line is fitted curve as the convolution of the other lines (see legends for the corresponding defects or transitions).

To reveal the effect of the liquid media on the product more clearly, the PL spectra were curve-fitted using six Gaussian functions similar to those previously reported in the literature.[6,8] As an example, Fig. 2(b) presents the results of curve-fitting for the PL spectrum of the sample prepared in

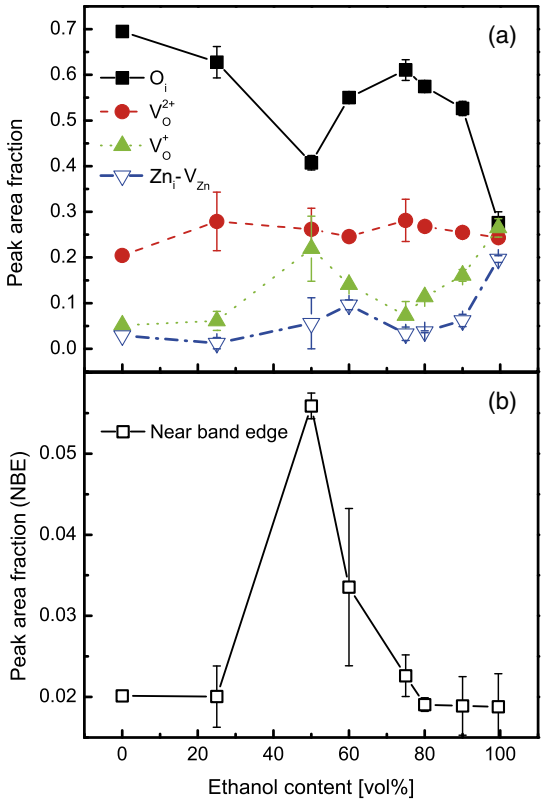

Fig. 3. (Color online) Area fractions of curve-fitted photoluminescence peaks corresponding to diverse defects as a function of ethanol concentration in liquid medium: (a) O_i, V_O^{2+}, V_O^+, and Zn_i–V_{Zn}; (b) near-band-edge emission. Lines are only given as guide to the eye.

75 vol % of ethanol. For simplicity, in the text below, the UV emission is referred to as the near-band-edge (NBE) emission, although it is known to come from several different origins. The main sources were most likely the free exciton and conduction-band-to-acceptor transitions,[33] since the experimentally detected UV emission was well fitted by two Gaussian peaks, thus implying two origins. As revealing such origins requires additional complex studies at very low temperatures,[33] the UV peak (as a sum of two Gaussian peaks) is simply treated below as the NBE emission. Meanwhile, the visible emission near 550 nm was curve-fitted as having four peaks at 478, 516, 569, and 629 nm. The three peaks at 516, 569, and 629 nm are assigned to singly-charged oxygen vacancies (V_O^+), doubly-charged oxygen vacancies (V_O^{2+}), and interstitial oxygen (O_i) defects, respectively.[2,6,9,10,12–14] The latter O_i defects are believed to be mainly located at the surface of ZnO NPs.[2] The peak at 478 nm (labeled as Zn_i–V_{Zn} peak below) was assigned to the donor-to-acceptor transitions, with interstitial Zn (Zn_i) and Zn vacancies (V_{Zn}) being the donor and acceptor, respectively.[2,6,34,35] The obtained area fractions of the peaks are shown in Fig. 3 as a function of ethanol volume fraction in liquid medium during NP preparation.

At ethanol concentrations in the liquid medium below 50 vol %, where the peaks of metallic Zn are not confirmed by XRD (see Fig. 1), the area fraction associated with the V_O^+ defects (green filled triangles) increases while that of the V_O^{2+} defects (red circles) slightly increases over ethanol concentration, as well seen in Fig. 3(a). This implies that the total number of oxygen-related vacancies increases as the

amount of stronger oxidizer, H_2O, decreases in the system. In agreement with the overall gradual increase in the density of oxygen vacancies, the area fraction of the O_i defects is seen in Fig. 3(a) (black filled squares) to decrease in the same ethanol concentration range (0–50 vol %). In parallel, the area fraction of the NBE emission increases [see Fig. 3(b)]. As the number of surface-related defects reduced, the UV emission related to the interband transition of the ZnO NPs was expected to increase, which is indeed seen in Fig. 3(b) (empty squares) at ethanol concentrations between 0 and 50 vol %. Relatively higher ratios of UV to visible emission in ZnO nanomaterials were previously reported to be indicative of their improved crystallinity.[18] This was explained by the interruption of the exciton UV emission via the trapping of electrons or holes at disorders in semiconducting materials with lower crystallinity.[18] Therefore, the combination of a minimum in surface defects [black squares in Fig. 3(a)] and maximum contribution of the NBE peak [Fig. 3(b)] in the NPs prepared at 50 vol % of ethanol permit to assume that ZnO NPs prepared in this liquid had improved crystallinity.

Interestingly, almost all PL trends in Figs. 3(a) and 3(b) change their behavior when the NPs are prepared in liquids with ethanol concentrations over 50 vol % (see Fig. 3). In accordance with Fig. 1, where peaks of metallic Zn clearly emerged in the XRD patterns of samples prepared in ethanol-rich media, it can be assumed that it was the appearance of this phase in ZnO NPs that drastically changed the situation. As a result, the behavior of PL emission of the materials prepared in ethanol-rich media is rather complex. As seen in Fig. 3(b), at 50 to 60 vol % of ethanol in the medium, the relative intensity of the NBE emission decreases along with that of the singly-charged oxygen vacancies [green triangles in Fig. 3(a)]. While the precise mechanisms are still to be revealed, the appearance of metallic Zn inside ZnO NPs is believed to lead to the dominance of surface-related defects over bulk ones, resulting in the recovery of the O_i defect density and the weakening of the NBE and V_O^+ emissions (black filled, black empty squares, and green filled triangles, respectively, in Fig. 3). The small peak observed in the Zn_i–V_{Zn} trend at ~60% [blue empty triangles in Fig. 3(a)] can be attributed to a density balance between the V_{Zn} (as acceptors) and Zn_i defects (as donors). As the amount of H_2O (as stronger oxidizer) in the medium decreases and metallic Zn phase emerges inside ZnO NPs, it is reasonable that the density of V_{Zn} decreases while that of Zn_i increases.[2,36]

At very high ethanol concentrations in the liquid media (75 to 99.5 vol %), the visible PL emission of the product NPs moves to the shorter-wavelength region as the NBE signal fraction decreases [Figs. 2(a) and 3(b)]. This should also be attributed to a gradually decreasing oxidation capability of the liquid mixture. Therefore, the signal fraction of the O_i defects, which has the largest area and thus is the most influential on the total signal strength, decreased. The use of such ethanol-rich environments with low oxidizing potential might also lead to an increase in the densities of singly-charged oxygen vacancies and Zn interstitials,[2,36] enhancing the V_O^+ and Zn_i–V_{Zn} related emission, though the increase of their emissions might be partially attributed to the reduction of the O_i defects.

The effect of medium pressure on the PL spectra of ZnO NPs produced via LAL in different water–ethanol mixtures

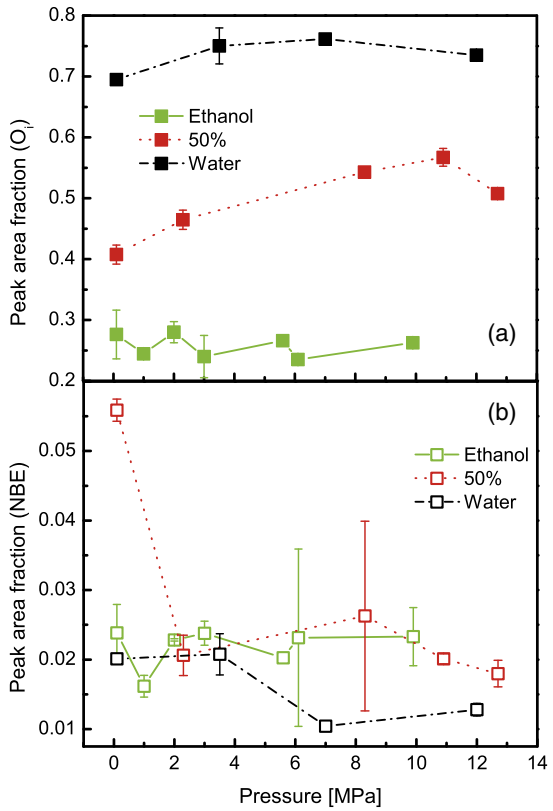

Fig. 4. (Color online) Area fractions of curve-fitted peaks assigned to (a) O_i and (b) NBE emission as a function of pressure. Ethanol content in the media: 99.5 vol % (green), 50 vol % (red), and 0 vol % (black symbols). Lines are only given as guide to the eye.

was also studied. Figures 4(a) and 4(b) show how the area fractions of the O_i (a) and NBE (b) related peaks changed as a function of externally-applied pressure for three ethanol concentrations (0, 50, and 99.5 vol %, respectively black, red and green symbols) in liquid media pressurized from 1 atm to 13 MPa. The area fractions of the other peaks (V_O^+, V_O^{2+}, and Zn_i–V_{Zn}) did not show any noticeable changes with pressure and thus are not shown.

It is well seen in Figs. 4(a) and 4(b) that with increasing pressure in pure water (black symbols) or water–ethanol mixtures (red symbols), both peaks related to the O_i (a) and NBE (b) defects demonstrate certain trends. In contrast, the use of ethanol as a medium for ablation did not allow for much control over the O_i defects [green filled squares in Fig. 4(a)]. This might be attributed to a relatively high amount of a metallic Zn phase in the product. In both water and water–ethanol media, with increase of pressure, the O_i area fraction increased [black and red squares in Fig. 4(a)], whereas the NBE area fraction decreased [black and red empty squares in Fig. 4(b)]. This trend is very likely to be owing to the shorter lifetimes of the cavitation bubble, where ablated Zn species react with the media and form ZnO NPs. Shorter lifetimes of the cavitation bubble were previously observed with pressure increase of the medium.[5,25,30,31] The quenching effect, which is characteristic of nanomaterials produced via LAL,[24,28,29] is expected to be even more rapid in the cavitation bubble with a shorter lifetime. This implies that in pressurized liquids the NPs should form even faster, which, e.g., was previously reported to give rise to smaller ZnO NPs prepared via LAL in neat water[5,25] as their agglomeration was

believed to be suppressed under such conditions. Thus, a higher density of surface defects can be expected as a result of a larger surface-to-volume ratio in such smaller particles formed at higher pressures. Furthermore, the rapid quenching at higher pressures is likely to cause more defects in the formed NPs. However, why it was only the O_i defect to follow this trend with pressure [black and red squares in Fig. 4(a)] still remains unanswered. The most remarkable drop is seen for the NBE emission observed in ZnO NPs laser-produced in water–ethanol mixtures [red empty squares in Fig. 4(b)], as the area fraction of the corresponding peak dropped down to zero at ~13 MPa. Since the ZnO NPs prepared in a similar water–ethanol mixture at 1 atm indicated the strongest UV emission [black empty squares in Fig. 3(b)], the pressure effect on such defects is visible.

In summary, the defects in ZnO nanoparticles prepared via laser ablation of the Zn target in various water–ethanol mixtures pressurized from 1 atm to 13 MPa were investigated by means of PL spectroscopy. The produced nanomaterials were also analyzed by X-ray diffractometry, revealing the appearance of metallic Zn, in addition to the main ZnO phase, in products ablated in media with ethanol content over 50%. The PL measurements demonstrated that both using different media for ablation and changing medium pressure significantly influenced the amount and nature of defects in the particles. At 50% of ethanol in the medium, the ZnO nanoparticles contained the small signal fraction of interstitial oxygen defects and emitted the strongest UV light, implying the product probably had the highest crystallinity. As the ethanol content in the liquid was more than 50%, metallic zinc emerged partially in the particles, resulting in more surface defects. The medium pressure was also found to affect the defects in ZnO. With the increase in pressure, the signal of oxygen defects increased while the near-band-edge related emission weakened. The effect of pressure was believed to be mainly associated with drastically shorter lifetimes of the cavitation bubble, where the ZnO nanoparticles form during laser ablation: as the quenching stage was much shorter and more rapid in pressurized media, this significantly influenced the defect nature in the produced nanostructures. Thus, both the use of media with different water–ethanol ratios, as well as external pressure, during laser ablation permit to control various defects produced in ZnO nanoparticles, helping tailor such materials for various applications.

Acknowledgments The work was financially supported by the Japan Society for the Promotion of Science (JSPS) and the Ministry of Education, Culture, Sports, Science and Technology, Japan (MEXT).

1) S. B. Zhang, S. H. Wei, and A. Zunger, Phys. Rev. B **63**, 075205 (2001).
2) A. Janotti and C. G. Van de Walle, Phys. Rev. B **76**, 165202 (2007).
3) Y. S. Fu, X. W. Du, S. A. Kulinich, J. S. Qiu, W. J. Qin, R. Li, J. Sun, and J. Liu, J. Am. Chem. Soc. **129**, 16029 (2007).
4) H. S. Desarkar, P. Kumbhakar, and A. K. Mitra, Laser Phys. Lett. **10**, 055903 (2013).
5) S. A. Kulinich, T. Kondo, Y. Shimizu, and T. Ito, J. Appl. Phys. **113**, 033509 (2013).
6) X. Y. Xu, C. X. Xu, Y. Lin, J. Li, and J. G. Hu, J. Phys. Chem. C **117**, 24549 (2013).
7) J. Song, S. A. Kulinich, J. Li, Y. Liu, and H. Zeng, Angew. Chem., Int. Ed. **54**, 462 (2015).
8) I. Thakur, S. Chatterjee, S. Swain, A. Ghosh, S. K. Behera, and Y. S. Chaudhary, New J. Chem. **39**, 2612 (2015).
9) B. Panigrahy, M. Asla, D. S. Misra, M. Ghosh, and D. Bahadur, Adv. Funct. Mater. **20**, 1161 (2010).
10) T. Taniguchi, K. Yamaguchi, A. Shigeta, Y. Matsuda, S. Hayami, T. Shimizu, T. Matsui, T. Yamazaki, A. Funatsu, Y. Makinose, N. Matsushita, M. Koinuma, and Y. Matsumoto, Adv. Funct. Mater. **23**, 3140 (2013).
11) Y. S. Fu, Y. F. Song, S. A. Kulinich, J. Sun, J. Liu, and X. W. Du, J. Phys. Chem. Solids **69**, 880 (2008).
12) P. Zhan, W. P. Wang, C. Liu, Y. Hu, Z. C. Li, Z. J. Zhang, P. Zhang, B. Y. Wang, and X. Z. Cao, J. Appl. Phys. **111**, 033501 (2012).
13) W. M. Kwok, A. B. Djurišić, Y. H. Leung, W. K. Chan, and D. L. Phillips, Appl. Phys. Lett. **87**, 093108 (2005).
14) P. S. Xu, Y. M. Sun, C. S. Shi, F. Q. Xu, and H. B. Pan, Nucl. Instrum. Methods Phys. Res., Sect. B **199**, 286 (2003).
15) J. Z. Song, S. A. Kulinich, J. Yan, Z. G. Li, J. P. He, C. X. Kan, and H. B. Zeng, Adv. Mater. **25**, 5750 (2013).
16) K. Kawabata, Y. Nanai, S. Kimura, and T. Okuno, Appl. Phys. A **107**, 213 (2012).
17) H. Usui, Y. Shimizu, T. Sasaki, and N. Koshizaki, J. Phys. Chem. B **109**, 120 (2005).
18) J. Zhao, L. Z. Hu, Z. Y. Wang, Y. Zhao, X. P. Liang, and M. T. Wang, Appl. Surf. Sci. **229**, 311 (2004).
19) M. Distaso, M. Mačković, E. Spiecker, and W. Peukert, Chem.—Eur. J. **20**, 8199 (2014).
20) K. K. Kim, D. Kim, S. K. Kim, S. M. Park, and J. K. Song, Chem. Phys. Lett. **511**, 116 (2011).
21) E. Chelnokov, M. Rivoal, Y. Colignon, D. Gachet, L. Bekere, and F. Thibaudau, Appl. Surf. Sci. **258**, 9408 (2012).
22) F. Mafuné, J. Kohno, Y. Takeda, and T. Kondow, J. Phys. Chem. B **104**, 9111 (2000).
23) E. Fazio, A. M. Mezzasalma, G. Mondio, F. Neri, and R. Saija, Appl. Surf. Sci. **272**, 30 (2013).
24) K. Y. Niu, J. Yang, S. A. Kulinich, J. Sun, H. Li, and X. W. Du, J. Am. Chem. Soc. **132**, 9814 (2010).
25) W. Soliman, N. Takada, N. Koshizaki, and K. Sasaki, Appl. Phys. A **110**, 779 (2013).
26) K. Y. Niu, J. Yang, S. A. Kulinich, J. Sun, and X. W. Du, Langmuir **26**, 16652 (2010).
27) R. Zamiri, A. Zkaria, H. Abbastabar Ahangar, M. Darroudi, A. Khorsand Zak, and G. P. C. Drummen, J. Alloys Compd. **516**, 41 (2012).
28) H. B. Zeng, X. W. Du, S. C. Singh, S. A. Kulinich, S. K. Yang, J. P. He, and W. P. Cai, Adv. Funct. Mater. **22**, 1333 (2012).
29) W. J. Qin, S. A. Kulinich, X. B. Yang, J. Sun, and X. W. Du, J. Appl. Phys. **106**, 114318 (2009).
30) M. Koizumi, S. A. Kulinich, Y. Shimizu, and T. Ito, J. Appl. Phys. **114**, 214301 (2013).
31) K. Sasaki, T. Nakano, W. Soliman, and N. Takada, Appl. Phys. Express **2**, 046501 (2009).
32) J. M. Cho, J. K. Song, and S. M. Park, Bull. Korean Chem. Soc. **30**, 1616 (2009).
33) W. Q. Peng, S. C. Qu, G. W. Cong, and Z. G. Wang, Appl. Phys. Lett. **88**, 101902 (2006).
34) B. Lin, Z. Fu, and Y. Jia, Appl. Phys. Lett. **79**, 943 (2001).
35) Y. W. Heo, D. P. Norton, and S. J. Pearton, J. Appl. Phys. **98**, 073502 (2005).
36) H. Zeng, W. Cai, J. Hu, G. Duan, P. Liu, and Y. Li, Appl. Phys. Lett. **88**, 171910 (2006).